Invited Paper

How to measure slow diffusion in yeast cell membranes

Jonas Ries*[a], Christian Klose*[b], Christiane Walch-Solimena[c] and Petra Schwille†[a]

[a]Biotechnologisches Zentrum, TU Dresden, Tatzberg 47-51, D-01307 Dresden, Germany
[b]MPI for Molecular Cell Biology and Genetics, Pfotenhauerstrasse 108, D-01307 Dresden, Germany
[c]Max Planck Society, Am Hofgarten 8, D-80539 München, Germany

ABSTRACT

Here we present two complementary methods for accurate diffusion measurements in yeast cell membranes. Fluorescence spreading after photobleaching analyzes the blurring of an initially sharp border between bleached and unbleached parts of the membrane. Two-focus scanning fluorescence correlation spectroscopy requires only a low concentration of labeled fluorophores and allows for very long measurement times due to correction for instabilities necessary to probe the slow diffusion in yeast plasma membranes. We apply these techniques to study the dynamics of different transmembrane proteins in the plasma membrane of the yeast *Saccharomyces cerevisiae*. The differences in the diffusion coefficients support the idea of co-existing membrane microdomains in the yeast plasma membrane.

Keywords: Diffusion, FRAP, fluorescence recovery after photobleaching, FCS, Gap1p, palmitoylation

INTRODUCTION

The plasma membrane of the yeast *Saccharomyces cerevisiae* is highly enriched in sphingolipids and sterols[1] which have been proposed to be able to form distinct membrane microdomains, so-called lipid rafts.[2] The lipids in these microdomains are present in a liquid-ordered phase (i.e. exhibit a high acyl chain order), in contrast to membranes in a liquid-disordered phase where the acyl chain order is more diffuse.

A remarkable characteristic of components of the yeast plasma membrane is their anomalously slow mobility in the plane of the membrane. Both proteins and lipids of the yeast plasma membrane exhibit an up to 40-fold lower diffusion coefficient than components of the plasma membrane of mammalian cells.[3,4] It has been suggested that this property of the yeast plasma membrane is at least in part due to the physical properties of the lipid bilayer since a block of synthesis of ergosterol (the major sterol in yeast) results in a 2-fold increase of diffusion. Furthermore, the slow mobility of yeast plasma membrane proteins and lipids does not depend on the structural integrity of the cell wall or the actin cytoskeleton.[4] Thus, diffusion coefficients of yeast plasma membrane proteins seem to depend partially on the lipid composition of the plasma membrane. However, diffusion behavior of a protein might also be influenced by its intrinsic properties that ensure a proper interaction with its lipid environment. For example, palmitoylation (the covalent attachment of palmitate, a C16:0 fatty acid, to a protein) is required for some transmembrane proteins in order to be associated with lipid rafts. Preventing their palmitoylation leads to their exclusion from lipid rafts, as has been shown for linker of activated T cells (LAT).[5] The inability to partition into a distinct membrane microdomain, i.e. to interact with a certain lipid environment, might result in an altered lateral diffusion. Indeed, raft proteins have been shown to diffuse faster than non-raft proteins in the apical plasma membrane of epithelial cells.[6] Therefore, determining diffusion coefficients for different plasma membrane proteins could reveal differences in their association to different membrane microdomains.

Previous studies on diffusion in yeast cell membranes have used fluorescence recovery after photobleaching (FRAP):[3,4] a region in the membrane is bleached and the recovery of membrane dyes or membrane associated fluorescent proteins is monitored. From the recovery time an approximate diffusion coefficient can be deduced. However, the relation between the recovery time and the diffusion coefficient depends in a non-trivial way on the shape of the bleached region. In addition, photobleaching during the monitoring of the recovery, finite bleaching

* these authors contributed equally to the work
† Corresponding author. Tel.: +49-351-46340328, Fax: +49-351-46340342, E-mail: petra.schwille@biotec.tu-dresden.de

Biophotonics: Photonic Solutions for Better Health Care, edited by
Jürgen Popp, Wolfgang Drexler, Valery V. Tuchin, Dennis L. Matthews,
Proc. of SPIE Vol. 6991, 69910W, (2008) · 1605-7422/08/$18 · doi: 10.1117/12.787043

times, cytosolic contributions, association to and dissociation from the membrane or instabilities of the sample corrupt the accuracy of FRAP.

Here we present two complementary methods for accurate measurement of diffusion coefficients in yeast membranes. Fluorescence spreading after photobleaching (FSAP), a variant of FRAP, analyzes the blurring of an initially sharp border between bleached and unbleached parts of the membrane.[7] This method is robust against most artifacts and allows direct extraction of diffusion coefficients without relying on a complex model. In addition, it allows to separate association/dissociation dynamics from diffusion. However, it requires a high concentration of fluorescent molecules in the membranes.

For low concentrations, two-focus scanning fluorescence correlation spectroscopy (FCS) measures diffusion coefficients on the single molecule level. Whereas standard confocal FCS is a popular method to study the dynamics of fluorophores in solution and is increasingly applied on model and cell membranes, it cannot be used on yeast cell membranes due to the extremely slow diffusion.[8] To gain sufficient statistical accuracy, the measurement time has to surpass the diffusion time $10^3 - 10^4$ fold. During this time (in yeast plasma membranes at least 30 min) the position of the detection volume with respect to the membrane would have to be stable with an accuracy of ≈ 100 nm. To prevent photobleaching, very low excitation powers have to be employed, resulting in a signal concealed by the dark counts of the detector. Scanning FCS,[9,10] on the other hand, allows to correct for instabilities and enables sufficiently long measurement times. In addition, high laser powers can be used to obtain a good signal to background ratio with a low risk of photobleaching. The use of two foci instead of one not only allows to directly extract the diffusion coefficient without a calibration measurement to determine the size of the detection area. It also helps to detect artifacts which arise from photobleaching, single bright events or residual instabilities. These artifacts can strongly affect the shape of the cross-correlation curve whereas they might not lead to a prominent deformation of the auto-correlation curve.

We apply fluorescence spreading after photobleaching in order to determine diffusion coefficients for three different C-terminally GFP-labeled yeast plasma membrane proteins: FusMidp, a chimeric single-spanning transmembrane protein, Gap1p, a palmitoylated amino acid permease containing 12 transmembrane domains and $\mathrm{Gap1^{C602G}p}$, a mutated Gap1p that lacks the palmitoylation site.[11,12] The diffusion coefficients will allow us to draw conclusions on whether the proteins of interest interact with different lipid environments. Of special interest is the question whether lack of palmitoylation affects the mobility of Gap1p in the plasma membrane resulting from an altered interaction with the lipid environment.

THEORY

Fluorescence spreading after photobleaching

By scanning a rectangular field of view with a high laser power, approx. half of the yeast cell can be bleached (see fig. 1a). Note that bleaching does not only occur in the focal plane, but also above and below. The border between the bleached and unbleached membrane part is initially sharp, but due to diffusion of fluorophores it blurs with time (fig. 1b). By analyzing the width of the transition at different time points, the diffusion coefficient can be deduced.

In the focal plane the diffusion can be described by an effective one-dimensional process with x being the coordinate along the membrane. For Brownian diffusion a fluorophore at the position x_0 at time $t = 0$ has a probability $p(x,t)$ to be found at position x at time t:

$$p(x, x_0, t) = \frac{1}{\sqrt{4\pi D t}} e^{-\frac{(x-x_0)^2}{4Dt}} \tag{1}$$

If a sharp profile is bleached at $x = x_s$, over time t diffusion of bright fluorophores into the dark part and of dark fluorophores into the bright part leads to a blurring of the border. The profile is then described by:

$$I(x,t) \propto \int_{x_s}^{\infty} p(x, x_0, t) dx_0 \propto \mathrm{erf}\left[\frac{x - x_0}{\sqrt{4Dt}}\right] + 1 \tag{2}$$

To extract a diffusion coefficient from the intensity profile $I(x,t)$, it is fitted with the error function to determine the width σ of the slope (fig. 1c):

$$I(x,t) = I_1 \mathrm{erf}\left[\frac{x - x_s}{\sigma(t)}\right] + I_0 \tag{3}$$

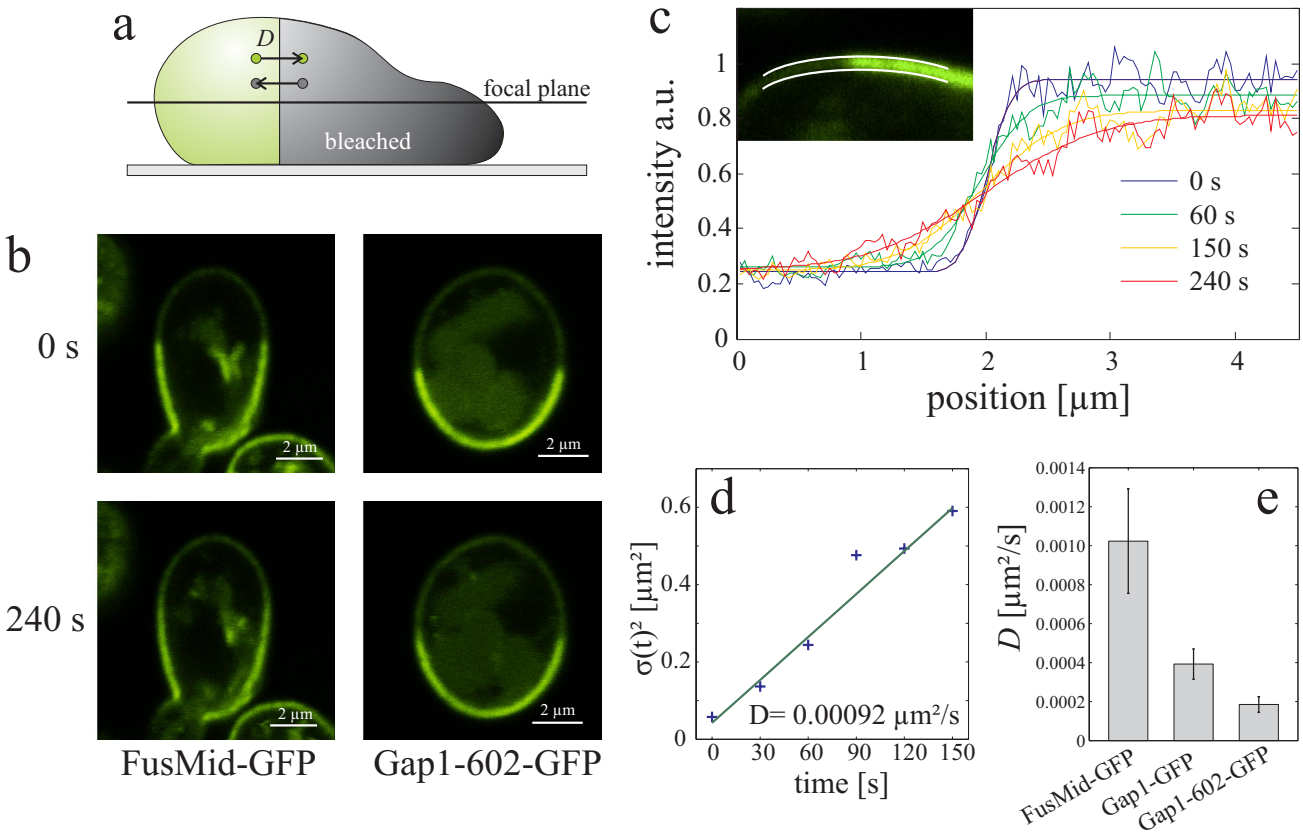

Figure 1. **Fluorescence spreading after photobleaching analysis in yeast cell membranes. a:** Sketch of the method. A large part of the yeast cell membrane is photobleached. Diffusion of unbleached fluorophores into the bleached parts and of bleached fluorophores into the unbleached parts results in a blurring of the border in time. **b:** Post-bleach images for FusMid-GFP and Gap1^{C602G}-GFP. Directly after the bleaching cycle the transition between bleached and unbleached parts is abrupt, after 240 seconds it is smooth for FusMid-GFP. Due to the slower diffusion, it is still steep for Gap1^{C602G}-GFP. **c:** Intensity profiles for FusMid-GFP for different times after the bleaching cycle and fits to eq. 3. The reduction of the maximum intensity is due to photobleaching. Inset: part of the image to reconstruct the intensity profile. **d:** Plot of $\sigma(t)^2$ vs. t and robust linear fit. From the slope the diffusion coefficient can be inferred. **e:** Average diffusion coefficients and 95% confidence intervals for FusMid-GFP, Gap1-GFP and Gap1^{C602G}-GFP from at least 20 individual measurements per sample. The difference between the diffusion coefficients is highly significant (students t-test: FusMid-GFP and Gap1-GFP: $p = 6 \cdot 10^{-5}$; FusMid-GFP and Gap1^{C602G}-GFP: $p = 5 \cdot 10^{-7}$; Gap1-GFP and Gap1^{C602G}-GFP: $p = 4 \cdot 10^{-5}$).

Due to the Gaussian shape of the bleaching laser beam and some diffusion during the bleaching time, even directly after the bleaching cycle the border is not completely sharp but exhibits an initial width σ_0. However, this profile is hardly distinguishable from a profile measured at time $t_0 = \sigma_0^2/4D$ after bleaching of a perfect step profile:

$$\sigma(t)^2 = 4D(t + t_0) = 4Dt + {\sigma_0}^2 \tag{4}$$

Therefore, the diffusion coefficient can be extracted from the slope of $\sigma(t)^2$ without knowledge of σ_0. A robust regression algorithm is less sensitive to outliers which can arise e.g. from cytosolic bright vesicles close to the membrane (fig. 1d).

Unwanted photobleaching during the acquisition of the time series decreases the signal to noise ratio, but does not affect the shape of the profiles. Therefore it is much less of a problem than in conventional FRAP. Note that binding/unbinding dynamics (e.g. endo- and exocytosis) do not change the shape of the profile but result in a recovery of the baseline I_0 in eq. 3, which can be used to deduce dynamic binding parameters.

Two-focus scanning FCS

In scanning FCS the detection volume is repeatedly scanned in a perpendicular way through a vertical membrane (fig. 2a). The individual line-scans can be arranged as a pseudo-image, where the vertical axis denotes the time. In this pseudo-image, the membrane is clearly visible. Due to instabilities, the position of the membrane is not constant in time (fig. 2b). These instabilities can be corrected for by shifting each line-scan so that the membrane forms a straight line (fig. 2c). For each scan, membrane contributions are added up to result in one point of the intensity trace (fig. 2d) which can be used to calculate the correlation curve (fig. 2e).

For calibration-free diffusion measurements with two-focus scanning FCS not only one, but two parallel lines with a distance d are repeatedly scanned through the membrane in an alternating fashion. The cross-correlation of the intensity traces corresponding to the two intersections is described by the following correlation function:[10]

$$G_x(\tau) = \frac{1}{C\pi S w_0^2}\left(1 + \frac{4D\tau}{w_0^2}\right)^{-1/2}\left(1 + \frac{4D\tau}{w_0^2 S^2}\right)^{-1/2}\exp\left(-\frac{d^2}{w_0^2 + 4D\tau}\right) \tag{5}$$

$S = w_z/w_0$ is the usual structure parameter. The auto-correlation function follows for $d = 0$. The triplet contribution can be neglected, since triplet times are in the range of microseconds and cannot be resolved with scanning FCS.

Once d is known, D and w_0 can be determined directly by fitting the data to eq. 5 without any additional calibration measurement. A global fit of the two auto-correlation functions and the cross-correlation function improves the accuracy.

Depletion of fluorophores due to photobleaching can be corrected for as described by Ries et al.,[13] allowing for long measurements even if the reservoir of fluorophores is limited, as is the case here.

MATERIALS AND METHODS

Fluorescence spreading after photobleaching

Measurements were performed with a Zeiss Confocor 3 (Zeiss, Jena, Germany) as follows: While focusing on the equatorial plane, half of the yeast cell was bleached with 120 µW for 4 seconds using the 488 nm laser line. One pre-bleach and post-bleach images (interval 30 s) were acquired in the APD-imaging mode with a laser power of 3 µW and a BP 505-610 emission filter. Photobleaching analysis was performed with software written MATLAB (MathWorks, Natick, MA). The membrane was identified in the pre-bleach image by approximating it locally around the bleached border with an ellipse. For all images, the intensity profile was inferred by adding up contributions of the membrane around the elliptical approximation (fig. 1c). Profiles were normalized to the pre-bleach profile to avoid artifacts due to inhomogeneities before fitting them to eq. 3. A robust linear regression algorithm was employed to infer the diffusion coefficient D from the measured $\sigma(t)$ (eq. 4). All measurements were performed at room temperature (22 ℃).

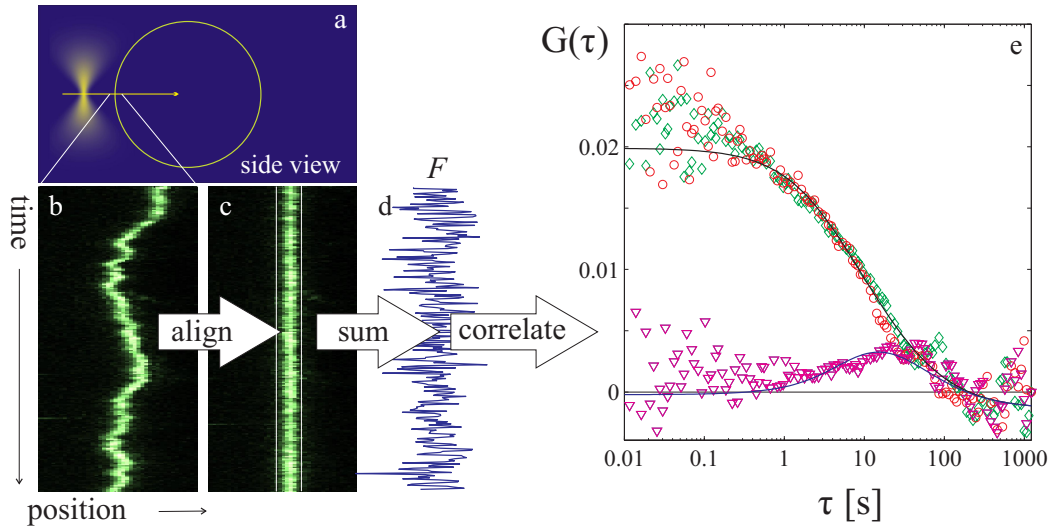

Figure 2. **Two-Focus Scanning FCS in yeast plasma membranes.** The detection volume is scanned repeatedly through the vertical membrane (a). Line scans are arranged under each other (b), the membrane is clearly visible. Membrane movements are corrected for (c) and membrane contributions from each scan are added up to result in the intensity trace (d) which can be correlated. e: Experimental auto- ($\circ$, $\diamond$) and cross-correlation ($\triangledown$) curves on FusMid-GFP in yeast cell membranes. Results from the fit to eq. 5: $C = 108 \pm 9$ µm^{-2}, $w_0 = 0.199 \pm 0.007$ µm, $D = 0.0023 \pm 0.0001$ µm^2/s. Distance between the foci $d = 0.34$ µm. Measurement parameters: Acquisition time: 30 min, excitation power P = 1 µW at 488 nm, scan speed v = 0.046 m/s.

Scanning FCS

Measurements were performed on an laser scanning microscope (LSM) Meta 510 system (Carl Zeiss, Jena, Germany) using a 40 × NA 1.2 UV-VIS-IR C Apochromat water-immersion objective, the 488 nm laser line and a home-built detection unit at the fiber output channel. A band-pass filter (HQ525/60M, AHF Analyse Technik, Tuebingen, Germany) was used behind a collimating achromat to reject the residual laser and background light. Another achromat (LINOS Photonics, Goettingen, Germany) with a shorter focal length was used to image the internal pinhole (diameter 60 µm) onto the aperture of the fiber connected to the avalanche photo diode (APD, PerkinElmer, Boston, MA). The photon arrival times were recorded in the photon mode of the hardware correlator Flex 02-01D (Correlator.com, Bridgewater, NJ).

The movement of the detection volume was controlled directly with the Zeiss LSM operation software. The frame mode with $N \times 2$ pixels was used to scan the two parallel lines. Their distance d was determined by repeatedly scanning over a film of dried fluorophores and measuring the distance between the bleached traces in a high resolution LSM-Image.

Data analysis was performed with software written in MATLAB (MathWorks, Natick, MA). The photon stream was binned in bins of 2 µs and arranged as a matrix such that every row corresponded to one line scan (fig. 2b). Movements of the membrane were corrected for by calculating the position of the maximum of a running average over several hundred line scans and shifting it to the same column. An average over all rows was fitted with a Gaussian and only the elements of each row between -2.5σ and 2.5σ were added to construct the intensity trace. The auto- and cross-correlation curves of the resulting intensity traces were computed with a multiple tau correlation algorithm and fitted with a nonlinear least squares fitting algorithm.

Plasmids, strains, growth conditions

The yeast wildtype strain BY4741 (*MATa his3*Δ *leu2*Δ *met15*Δ *ura3*Δ; from EUROSCARF) was transformed with DNA fragments containing *HIS3*, *LEU2* and *MET15* genes in order to obtain RY17 (*MATa ura3*Δ), a strain prototrophic for amino acids. Deletion of *GAP1* in RY17 according to Janke et al.[14] yielded RY38 (*MATa gap1::hphNTI ura3*Δ). A construct expressing FusMid-GFP from the *GALs* promotor pTPQ55 was kindly provided by Tomasz Proszinsky.[11] Gap1-GFP expressed from the *GAP1* promotor (pCK230) was a kind gift of

Chris Kaiser.[15] A plasmid expressing Gap1-GFP lacking the palmitoylation site (Gap1^{C602G}-GFP, pR26) was obtained by site directed mutagenesis of pCK230 using QuikChange XL Kit from Stratagene (La Jolla, CA, USA).

Cells (RY17) carrying pTPQ55 were grown in selective medium with 2% raffinose. Expression of FusMid-GFP was induced by addition of 2% galactose (final concentration) for 3 h. Cells (RY38) containing plasmids encoding wildtype or mutant Gap1-GFP (pCK230 or pR26, respectively) were grown in minimal medium supplemented with 3% glucose and 40 mM $(NH_4)_2SO_4$ as single nitrogen source. For diffusion measurements cells were attached to the bottom of chambered glass slides (Roth, Karlsruhe, Germany) by using concanavalin A as described.[4]

RESULTS AND DISCUSSION

Fig. 1b shows post-bleach images for the proteins FusMid-GFP and Gap1^{C602G}-GFP, respectively. The transition between bleached and unbleached parts is rather abrupt for the images taken directly after the bleaching cycle. 240 seconds later, the transition is smooth for FusMid-GFP, for Gap1^{C602G}-GFP the border is still clearly visible, indicating slower diffusion. Fig. 1d reports the mean values and 95% confidence intervals of measured diffusion coefficients for FusMid-GFP, Gap1-GFP and Gap1^{C602G}-GFP, respectively. The differences between the three proteins are highly significant with p-values from the t-test below 10^{-4}. We found that the spread among individual cells was significantly larger than the precision of our technique, indicating a strong heterogeneity among the cells.

Fig. 2e shows results of a typical two-focus scanning FCS measurement on FusMid-GFP in yeast plasma membranes. The diffusion coefficient was found to be $D = 0.0023$ $\mu m^2/s$, the distance between the foci was previously determined to be $d = 340$ nm.

The chimeric protein FusMid-GFP served as an experimental control proving the validity of the diffusion coefficients determined by fluorescence spreading after photobleaching (FSAP) and two-focus scanning FCS. Due to the large spread in the diffusion coefficients the result obtained with two-focus FCS is within the range measured with FSAP. However, we found that two-focus scanning FCS measurements resulted on average in larger diffusion coefficients than FSAP. The reason is that, for a given measurement time, correlation curves for slow diffusion exhibit more noise and might more easily be discarded as bad curves. In addition, too short measurement times lead to a bias towards faster diffusion.[8] If a high concentration of fluorescent molecules can be achieved, FSAP is therefore preferable to two-focus scanning FCS. The diffusion coefficients determined for FusMid-GFP with both techniques are in agreement with previously reported values for single-spanning yeast plasma membrane proteins acquired by conventional FRAP ($D \approx 0.0025$ $\mu m^2/s$).[4] These results confirm that these techniques are adequate methods to determine diffusion rates of fluorescently labeled proteins in the yeast plasma membrane.

The 12-spanning transmembrane protein Gap1-GFP shows a more than two-fold slower diffusion than FusMid-GFP (fig. 1d). Since the diffusion depends on particle size, i.e. larger particles diffuse slower than smaller ones, we speculate that this might be due to the differences in the size of the membrane-spanning segments of the proteins (1 vs. 12 transmembrane domains). Surprisingly, the unpalmitoylated mutant Gap1^{C602G}-GFP diffuses about two times slower than the palmitoylated Gap1-GFP. This result might be explained by different scenarios. One possibility is that lack of palmitoylation of Gap1^{C602G}-GFP could lead to misfolding of the protein due to its inability to associate with the sterol- and sphingolipid-rich lipid environment of the yeast plasma membrane. Such a situation has been reported for Gap1 synthesized in the absence of sphingolipid biosynthesis leading to an aberrant conformation and non-functionality.[16] Misfolding might lead to aggregation of the protein resulting in reduced diffusion as has been shown for the mammalian protein Gas3/PMP22 in the endoplasmatic reticulum (ER).[17] However, activity measurements revealed that unpalmitoylated Gap1p is functional (our unpublished data), arguing against misfolding. We therefore favor an alternative explanation that bases on the fact that Gap1p is a raft protein.[18] The finding that unpalmitoylated Gap1^{C602G}p diffuses slower than palmitoylated Gap1p suggests that it partitions preferentially into an alternative, possibly non-raft phase. Similar differences between diffusion coefficients of raft and non-raft proteins have been reported for the apical plasma membrane of epithelial cells.[6] This idea is supported by the fact that several transmembrane proteins require palmitoylation for their association to lipid rafts like for example LAT.[5] However, so far it has not been shown whether palmitoylation of Gap1p has a similar function. Furthermore, although a domain-like

organization of the yeast plasma membrane has been suggested, there is no evidence for a non-raft phase.[16, 19–21] Future work will reveal whether palmitoylation of the multi-spanning transmembrane protein Gap1p is required for its association to lipid rafts and whether the lower mobility of unpalmitoylated Gap1^{C602G}p can indeed be attributed to a partitioning into a non-raft lipid environment.

CONCLUSION

We applied two novel complementary techniques to measure the slow diffusion of proteins in yeast plasma membranes. Fluorescence spreading after photobleaching allows for direct measurements of diffusion coefficients and is robust against most artifacts. Two-focus scanning FCS can be employed even for a minimal concentration of labeled proteins. The application of FSAP on the single-spanning transmembrane protein FusMidp, the multi-spanning palmitoylated Gap1p and the unpalmitoylated mutant Gap1^{C602G}p revealed differences in their diffusion coefficient. These differences in the diffusion behavior might be caused by differences in the topology of the proteins (i.e. number of transmembrane domains) and/or partitioning into alternative membrane microdomains. Further biochemical studies will help to dissect the molecular events leading to the observed differences in the diffusion of integral proteins of the yeast plasma membrane.

ACKNOWLEDGMENTS

We thank Tomasz Proszinsky and Chris Kaiser for providing plasmids and Robin Klemm for helpful comments on the manuscript.

REFERENCES

[1] E. Zinser and G. Daum, "Isolation and biochemical characterization of organelles from the yeast, saccharomyces cerevisiae," *Yeast* **11**, pp. 493–536, May 1995.

[2] K. Simons and E. Ikonen, "Functional rafts in cell membranes," *Nature* **387**, pp. 569–572, Jun 1997.

[3] M. Greenberg and D. Axelrod, "Anomalously slow mobility of fluorescent lipid probes in the plasma membrane of the yeast saccharomyces cerevisiae," *J Membr Biol* **131**(2), pp. 115–27, 1993.

[4] J. Valdez-Taubas and H. Pelham, "Slow diffusion of proteins in the yeast plasma membrane allows polarity to be maintained by endocytic cycling," *Curr Biol* **13**, pp. 1636–1640, Sept. 2003.

[5] W. Zhang, R. P. Trible, and L. E. Samelson, "Lat palmitoylation: its essential role in membrane microdomain targeting and tyrosine phosphorylation during t cell activation," *Immunity* **9**, pp. 239–246, Aug 1998.

[6] D. Meder, M. J. Moreno, P. Verkade, W. L. C. Vaz, and K. Simons, "Phase coexistence and connectivity in the apical membrane of polarized epithelial cells," *Proc Natl Acad Sci U S A* **103**, pp. 329–334, Jan 2006.

[7] M. Loose, E. Fischer-Friedrich, J. Ries, K. Kruse, and P. Schwille, "Spatial regulators for bacterial cell division self-organize into surface waves in vitro," *Science* , p. (in press), 2008.

[8] J. Ries and P. Schwille, "New concepts for fluorescence correlation spectroscopy on membranes," *Phys Chem Chem Phys* , p. doi: 10.1039/b718132a, 2008.

[9] Q. Ruan, M. Cheng, M. Levi, E. Gratton, and W. Mantulin, "Spatial-temporal studies of membrane dynamics: scanning fluorescence correlation spectroscopy (sfcs)," *Biophys J* **87**, pp. 1260–1267, Aug. 2004.

[10] J. Ries and P. Schwille, "Studying slow membrane dynamics with continuous wave scanning fluorescence correlation spectroscopy," *Biophys J* **91**, pp. 1915–1924, Sep 2006.

[11] T. J. Proszynski, R. W. Klemm, M. Gravert, P. P. Hsu, Y. Gloor, J. Wagner, K. Kozak, H. Grabner, K. Walzer, M. Bagnat, K. Simons, and C. Walch-Solimena, "A genome-wide visual screen reveals a role for sphingolipids and ergosterol in cell surface delivery in yeast," *Proc Natl Acad Sci U S A* **102**, pp. 17981–17986, Dec 2005.

[12] A. F. Roth, J. Wan, A. O. Bailey, B. Sun, J. A. Kuchar, W. N. Green, B. S. Phinney, J. R. Yates, and N. G. Davis, "Global analysis of protein palmitoylation in yeast," *Cell* **125**, pp. 1003–1013, Jun 2006.

[13] J. Ries, S. Chiantia, and P. Schwille, "Fast and accurate measurement of diffusion coefficients and concentrations on flat membranes with line-scan fcs," *(in preparation)* , 2008.

[14] C. Janke, M. M. Magiera, N. Rathfelder, C. Taxis, S. Reber, H. Maekawa, A. Moreno-Borchart, G. Doenges, E. Schwob, E. Schiebel, and M. Knop, "A versatile toolbox for pcr-based tagging of yeast genes: new fluorescent proteins, more markers and promoter substitution cassettes," *Yeast* **21**, pp. 947–962, Aug 2004.

[15] S. B. Helliwell, S. Losko, and C. A. Kaiser, "Components of a ubiquitin ligase complex specify polyubiquitination and intracellular trafficking of the general amino acid permease," *J Cell Biol* **153**, pp. 649–662, May 2001.

[16] E. Lauwers, G. Grossmann, and B. Andre, "Evidence for coupled biogenesis of yeast gap1 permease and sphingolipids: essential role in transport activity and normal control by ubiquitination," *Mol Biol Cell* **18**, pp. 3068–3080, Aug 2007.

[17] A. Fontanini, R. Chies, E. L. Snapp, M. Ferrarini, G. M. Fabrizi, and C. Brancolini, "Glycan-independent role of calnexin in the intracellular retention of charcot-marie-tooth 1a gas3/pmp22 mutants," *J Biol Chem* **280**, pp. 2378–2387, Jan 2005.

[18] E. Lauwers and B. Andre, "Association of yeast transporters with detergent-resistant membranes correlates with their cell-surface location," *Traffic* **7**, pp. 1045–1059, Aug 2006.

[19] G. Grossmann, M. Opekarova, J. Malinsky, I. Weig-Meckl, and W. Tanner, "Membrane potential governs lateral segregation of plasma membrane proteins and lipids in yeast," *EMBO J* **26**, pp. 1–8, Jan 2007.

[20] K. Malinska, J. Malinsky, M. Opekarova, and W. Tanner, "Visualization of protein compartmentation within the plasma membrane of living yeast cells," *Mol Biol Cell* **14**, pp. 4427–4436, Nov 2003.

[21] K. Malinska, J. Malinsky, M. Opekarova, and W. Tanner, "Distribution of can1p into stable domains reflects lateral protein segregation within the plasma membrane of living s. cerevisiae cells," *J Cell Sci* **117**, pp. 6031–6041, Dec 2004.